scientific reports

Check for updates

OPEN

Role of galectin-9 in the development of gestational diabetes mellitus

Haya Hamed Hassan Albuayjan[1], Mayu Watanabe[1], Ryosuke Sugawara[1], Eri Katsuyama[1,3], Koki Mise[1], Yukiko Oi[1], Ayaka Kanno[1], BoXuan Yang[1], Toshihisa Tahara[1], Ichiro Nojima[1], Atsuko Nakatsuka[1], Jun Eguchi[1], Jota Maki[2], Eriko Eto[2], Kei Hayata[2], Hisashi Masuyama[2] & Jun Wada[1]✉

Galectin-9 (Gal-9) is highly expressed in trophoblasts in placenta. Interaction between Gal-9 and T-cell immunoglobulin and mucin-domain containing-3 (Tim-3) is important for the differentiation of tissue resident natural killer (trNK) cells in placenta and maintenance of normal pregnancy. Furthermore, the enhanced maternal systemic inflammation associated with increased proinflammatory cytokines in preeclampsia is mediated by enhanced interaction between Gal-9 and Tim-3. However, the role of Gal-9 in gestational diabetes (GDM) remains unexplored. Plasma Gal-9 levels were elevated at 3rd trimester in pregnant women with GDM and positively correlated with placenta and newborn weight. *Lgals9* knockout pregnant mice fed with high fat diet (HFD KO) demonstrated maternal glucose intolerance and fetus macrosomia compared with controls (HFD WT). In HFD KO, increased proliferating cells, reduced apoptosis, and autophagy impairment were observed in junctional zones. The number of trNK cells and percentage of Tim-3 + trNK increased, while early apoptosis percentage in Tim-3 + trNK was reduced in placenta of HFD KO. The elevation of plasma Gal-9 may be a biomarker for prediction of maternal glucose intolerance and fetal macrosomia in pregnant women with GDM and Gal-9 functions as a compensation factor for GDM by inducing apoptosis in Tim-3 + trNK cells.

Gestational diabetes mellitus (GDM) is a pregnancy-related disorder characterized by glucose intolerance that arises during gestation. Affecting 5–10% of pregnancies worldwide[1], GDM significantly increases the risks of obstetric and neonatal complications such as higher infant birthweight, i.e. macrosomia. These complications are also recognized as risk factors for future cardiometabolic diseases in both mothers and offsprings, including type 2 diabetes, obesity and cardiovascular diseases[2]. However, the precise molecular mechanism for the development of GDM is still unraveled.

Galectins are a family of 15 members of β-galactoside binding lectins and share a highly conserved carbohydrate binding domain. Recently, it has been discovered that galectins are highly expressed at the maternal-fetal interface and involved in a variety of functions such as maternal-fetal immune tolerance, angiogenesis, trophoblast invasion and placental development during normal pregnancy. It further arouses the interests of researchers toward the possible roles of galectins in abnormal and pathological pregnancies[3]. Among the galectin family members, galectin-9 (Gal-9) was discovered as an inducer of apoptosis of thymocytes[4] and it also provokes apoptosis of activated Th1 and Th17 cells to induce T cell immune tolerance by binding to T-cell immunoglobulin and mucin-domain containing-3 (Tim-3) as a ligand[5].

In mouse normal pregnancy, Gal-9 is highly expressed in murine spongiotrophoblasts and decidual regulatory T cells (Tregs)[6], and the predominant Gal-9 splice variant (LGALS D5) downregulates IFN-γ production in decidual NK (dNK) cells, which may limit Th1 cell number[7]. In pathological pregnancies like spontaneous miscarriage, lower mRNA levels of Gal-9 in murine placenta[7], reduced expression of Tim-3 in dNK cells, decreased Th2 cytokine and increased Th1 cytokine levels in Tim-3 + dNK cells were observed in mouse models[8]. It suggests that the impairment of Gal-9/Tim-3 pathway results in an enhanced systemic inflammatory response. In addition to the immunological effects, Gal-9 also affects the trophoblast function in pregnancy. For

[1]Department of Nephrology, Rheumatology, Endocrinology and Metabolism, Okayama University Graduate School of Medicine, Dentistry and Pharmaceutical Sciences, Okayama University, 2-5-1 Shikata-cho, Kita-ku, Okayama 700-8558, Japan. [2]Department of Obstetrics and Gynecology, Okayama University Graduate School of Medicine, Dentistry and Pharmaceutical Sciences, Okayama University, Okayama, Japan. [3]Faculty of Health Science, Okayama University Medical School, Graduate School of Health Sciences, Okayama University, Okayama, Japan. ✉email: junwada@okayama-u.ac.jp

example, the exogenous rat Gal-9 administration alleviates the preeclampsia-like manifestations characterized by insufficient trophoblast cell invasion and impaired spiral artery remodeling in a rat model of preeclampsia induced by LPS by upregulating Tim-3 expression in decidual macrophages[9].

In human, Gal-9 expressed in primary trophoblasts induces transformation of peripheral NK cells to dNK-like cells via interaction with Tim-3, suggesting Gal-9/Tim-3 signal is important for the regulation of dNK cell function and maintenance of a normal pregnancy[10]. Furthermore, Gal-9/Tim-3 pathway has been implicated in the maternal systemic inflammation in early-onset of preeclampsia[5]. Decreased expression of Tim-3 in T cells, cytotoxic T cells, NK cells and $CD56^{dim}$ NK cells, while notably increased frequency of Gal-9 positive cells in each investigated lymphocyte population were observed in the case of early-onset preeclamptic patients[11]. The Tim-3 and Gal-9 were upregulated in decidual tissues in preeclampsia associated with increased levels of Th1 and Th17 cytokines[12]. Recently, contradictory results have been reported that trophoblast-derived Gal-9 activates $CD11c^{high}$ subpopulation of decidual macrophages (dMphi) that inhibits spiral artery remodeling in preeclampsia[8]. Gal-9 administration in preeclampsia mouse models induces preeclampsia-like phenotypes with increased $CD11c^{high}$ dMphi and defective spiral arteries, whereas galectin-9 blockade or macrophage-specific CD44 deletion prevents such phenotypes[8].

Although there are several reports of Gal-9 as a biomarker and therapeutic target in preeclampsia, there are no reports of the role of Gal-9 in GDM. In current studies, we aimed to investigate the role of Gal-9 in GDM by performing clinical observation study in the women with GDM and conducting animal experiments in B6-$Lgals9^{tm1glp}$ (KO) pregnant female mice fed with high fat diet (HFD). By the recent single cell sequencing, 3 subsets of dNK cells (dNK1, dNK2, dNK3) were discovered, these subsets co-express the tissue-resident markers such as CD49a[13], and we evaluated the population of tissue resident NK (trNK) cells in murine placenta. In addition to trNK cell profile, we also investigated autophagy, since Gal-9 maintains p62-dependent autophagic degradation of NOD-, LRR-, and pyrin domain-containing protein 3 (NLRP3)[14] and autophagic function co-operating with lysosomes by binding to lysosome-associated membrane protein 2 (LAMP2)[15].

Results

Expression of Gal-9 in the pregnant women with NGT and GDM

In the women with GDM, body mass index (BMI) and blood pressure were significantly higher throughout the pregnant period (Table 1). In human placenta tissue, *LGALS9* mRNA was abundantly expressed in the chorion layers compared to decidua in the women with both NGT and GDM (Fig. 1A). Plasma Gal-9 levels in non-pregnant women ($n=10$, 36.0 ± 3.42 years old) were 0.76 ± 0.15 ng/mL and lower than pregnant women with NGT and GDM. In GDM, plasma Gal-9 levels increased at 3rd trimester (2.01 ± 0.92 ng/mL) and they were higher than those of NGT (1.28 ± 0.51 ng/mL) ($P=0.014$). In GDM, plasma Gal-9 levels immediately declined after birth (1.16 ± 0.48 ng/mL) ($P=0.004$) (Fig. 1B; Table 1). In NGT, plasma Gal-9 levels at 2nd trimester revealed strong negative correlation with neonatal birth weight (BW) (r=-0.59, $P=0.021$), at 3rd trimester moderate correlation (r=-0.47, $P=0.053$), and after delivery weak correlation (r=-0.31, $P=0.142$). In GDM, plasma Gal-9 levels at 3rd trimester demonstrated negative correlation with HDL-C (r= -0.59, $P=0.013$) and positive correlation with HbA1c ($r=0.333$, $P=0.104$), placental weight ($r=0.53$, $P=0.014$), and neonatal BW ($r=0.50$, $P=0.021$), suggesting Gal-9 may have certain critical roles in metabolic abnormalities in GDM (Fig. 1C, D, and Supplementary Fig. 1). Plasma Gal-9 levels did not show significant correlations with other clinical parameters in both NGT and GDM (Supplementary Fig. S1).

Phenotypes and glucose metabolism in HFD KO pregnant mice

Eight-week-old female mice were randomly assigned to SFD and HFD groups and they were mated with male C57BL/6J mice at 12 weeks of age (Fig. 2A). Body weight in HFD KO mice at GD7 (21.18 ± 0.69 g) was significantly lower than HFD WT mice (25.71 ± 2.43) ($P=0.0005$). Similarly, the body weight in SFD KO mice at GD14 (24.23 ± 1.09) was lower than SFD WT (28.41 ± 4.68) ($P=0.0025$) (Fig. 2B). In GTT at GD14, blood glucose levels at 2 h after the glucose injection were significantly higher in HFD KO mice (257.7 ± 40.1 mg/dL) compared with HFD WT (154.6 ± 42.7 mg/dL) ($P=0.0017$) (Fig. 2C) and area under the curve (AUC) was also significantly higher in HFD KO mice. However, there were no significant differences in insulin levels in GTT (Fig. 2C). At GD14, HOMA-β and insulinogenic index were lower in HFD KO compared with HFD WT, but they were not statistically significant (Supplementary Fig. 2A, B). In ITT at GD16, the elevation of blood glucose levels was observed in HFD KO compared with HFD WT without statistically significant differences (Fig. 2D). At GD19, fasting serum insulin levels were higher in HFD KO (9.50 ± 5.46 μIU/mL) compared with HFD WT (6.59 ± 0.65 μIU/mL) without statistically significant differences (Fig. 2D) and progesterone levels were unaltered (Supplementary Fig. S2C). The data suggested that glucose intolerance with mild insulin secretion impairment and mild insulin resistance. Among various organs of the pregnant mice at GD19, there were no significant differences in placenta weight. Although the liver weight in HFD KO (1.31 ± 0.22 g) was lower than HFD WT mice (1.49 ± 0.24 g), it did not reach statistically significant levels ($P=0.63$). The ovarian fat weight was significantly lower in HFD KO (0.10 ± 0.04 g) than in HFD WT mice (0.17 ± 0.06 g) ($P=0.05$). The fetus weight at GD19 from HFD KO (1.34 ± 0.12 g) was significantly higher than HFD WT mice (0.96 ± 0.17 g) ($P=0.029$) (Fig. 2E and Supplementary Fig. S3A).

Cell proliferation, apoptosis and autophagy in placenta of HFD KO pregnant mice

Immunohistochemistry of Gal-9 demonstrated the intracellular and cell-surface expression in trophoblast giant cells (TGC; red arrows) and spongiotrophoblast cells (SP; yellow arrows) (Fig. 3A). Gal-9 protein levels in placenta were also confirmed by Western blot analysis. Densitometric analyses revealed that protein levels of Gal-9 in HFD KO were reduced to ~37% of the HFD WT mice (Fig. 3B, Supplementary Figs. S4 and S5). *Lgals9* mRNA expression showed a tendency to increase in placenta, ovarian fat and liver tissues of HFD WT

	NGT (*n*=14)	GDM (*n*=19)	*P* value
Age (years)	36.4 ± 3.6	34.7 ± 5.7	0.34
Pre-gestational BMI (kg/m^2)	21.8 ± 3.0	26.7 ± 4.5	0.0015
BMI at 2nd trimester (kg/m^2)	26.4 ± 3.8	30.7 ± 5.9	0.037
BMI at 3rd trimester (kg/m^2)	24.7 ± 2.8	28.3 ± 4.2	0.009
BMI after delivery (kg/m^2)	23.7 ± 2.8	27.3 ± 3.9	0.009
Blood pressure at 2nd trimester	107.4 ± 13.0	117.0 ± 10.0	0.045
Blood pressure at 3rd trimester	107.1 ± 10.5	116.8 ± 13.2	0.032
Blood pressure after delivery	110.4 ± 7.6	120.3 ± 12.7	0.016
Gestational weight gain (kg)	7.3 ± 3.2	3.2 ± 3.8	0.003
Gal-9 at 2nd trimester (ng/mL)	1.03 ± 0.39	1.08 ± 0.38	0.789
Gal-9 at 3rd trimester (ng/mL)	1.28 ± 0.51	2.01 ± 0.92	0.014
Gal-9 after delivery (ng/mL)	1.43 ± 0.71	1.16 ± 0.48	0.210
HbA1c at 2nd trimester (%)	5.24 ± 0.52	5.40 ± 0.45	0.491
HbA1c at 3rd trimester (%)	5.56 ± 0.35	5.73 ± 0.50	0.281
HbA1c after delivery (%)	5.32 ± 0.39	5.69 ± 0.66	0.094
T-Cho at 2nd trimester (mg/dL)	272.8 ± 44.4	239.9 ± 60.4	0.154
T-Cho at 3rd trimester (mg/dL)	297.8 ± 44.4	258.6 ± 53.8	0.047
T-Cho after delivery (mg/dL)	244.0 ± 49.4	215.6 ± 36.3	0.099
LDL-C at 2nd trimester (mg/dL)	152.5 ± 30.9	131.7 ± 42.9	0.198
LDL-C at 3rd trimester (mg/dL)	170.8 ± 38.4	138.7 ± 44.9	0.054
LDL-C after delivery (mg/dL)	138.2 ± 32.4	114.8 ± 29.4	0.059
HDL-C at 2nd trimester (mg/dL)	83.2 ± 9.9	72.9 ± 10.8	0.030
HDL-C at 3rd trimester (mg/dL)	79.6 ± 9.3	70.3 ± 14.9	0.063
HDL-C after delivery (mg/dL)	64.8 ± 15.4	57.4 ± 11.7	0.173
TG at 2nd trimester (mg/dL)	216.5 ± 71.2	202.9 ± 68.4	0.658
TG at 3rd trimester (mg/dL)	318.4 ± 86.0	309.7 ± 170.2	0.869
TG after delivery (mg/dL)	207.0 ± 73.6	204.3 ± 130.1	0.426
WBC at 2nd trimester (10^3/μL)	9.50 ± 2.10	9.63 ± 2.75	0.882
WBC at 3rd trimester (10^3/μL)	8.73 ± 2.38	8.54 ± 2.76	0.838
WBC after delivery (10^3/μL)	7.96 ± 2.50	8.49 ± 2.33	0.535
RBC at 2nd trimester (10^6/μL)	3.74 ± 0.4	4.02 ± 0.4	0.051
RBC at 3rd trimester (10^6/μL)	3.88 ± 0.3	4.13 ± 0.4	0.061
RBC after delivery (10^6/μL)	3.41 ± 0.4	3.53 ± 0.6	0.529
Hemoglobin at 2nd trimester (g/dL)	11.2 ± 0.9	12.1± 0.9	0.008
Hemoglobin at 3rd trimester (g/dL)	11.0 ± 1.2	11.8 ± 0.9	0.024
Hemoglobin after delivery (g/dL)	9.6 ± 1.2	9.8 ± 1.2	0.690
Hct at 2nd trimester (%)	34.2 ± 2.4	36.7 ± 2.3	0.006
Hct at 3rd trimester (%)	34.2 ± 3.1	36.4 ± 2.5	0.025
Hct after delivery (%)	30.5 ± 3.6	30.7 ± 3.5	0.842
Plt at 2nd trimester (10^3/μL)	273 ± 52	266 ± 48	0.717
Plt at 3rd trimester (10^3/μL)	258 ± 58	255 ± 46	0.877
Plt after delivery (10^3/μL)	236 ± 92	264 ± 64	0.313
AST after delivery (U/L)	25.5 ± 20.6	19.6 ± 12.3	0.314
ALT after delivery (U/L)	21.3 ± 13.5	13.3 ± 8.3	0.044
LDH after delivery (U/L)	272.3 ± 127.4	216.5 ± 76.0	0.126
CRP after delivery (mg/dL)	2.47 ± 1.58	2.31 ± 1.43	0.768
D-dimer after delivery (μg/mL)	5.71 ± 6.01	5.00 ± 5.41	0.725
Continued			

	NGT (*n*=14)	GDM (*n*=19)	*P* value
Gestational age of Delivery (weeks)	38.5 ± 1.2	38.2 ± 1.9	0.575
Placenta weight (g)	573.8 ± 70.6	541.7 ± 95.3	0.314
C-peptide (UCB) (ng/ml)	0.77 ± 0.19	0.95 ± 0.25	0.076
Neonatal body weight (g)	3117 ± 359	2944 ± 621	0.363
Neonatal plasma glucose (mg/dL)	62.3 ± 10.8	64.5 ± 16.0	0.676

Table 1. Clinical characteristics of pregnant women with normal glucose tolerance (NGT) and gestational diabetes mellitus (GDM). Data are shown as mean ± SD and analyzed by Student *t*-test. *BMI* body mass index, *Gal-9* galectin-9, *HbA1c* hemoglobin A1c, *T-Cho* total cholesterol, *LDL-C* low-density lipoprotein-cholesterol, *HDL-C* high-density lipoprotein-cholesterol, *TG* triglycerides, *WBC* white blood cells, *RBC* red blood cells, *Hct* hematocrit, *Plt* platelets, *AST* aspartate aminotransferase, *ALT* alanine aminotransferase, LDH lactate dehydrogenase, *CRP* C-reactive protein, *D-dimer* fibrin degradation product D-dimer, *C-peptide (UCB)* C-peptide in umbilical cord blood.

compared with SFD WT pregnant mice (Fig. 3C and Supplementary Fig. S3B). Since Gal-9 is involved in cell cycle regulation by inducing apoptosis and proliferation of the cells such as activated Th1 cells and macrophages, we investigated the status of proliferation and apoptosis in placenta tissues. In placenta derived from HFD KO pregnant mice, elevated number of PCNA positive cells and higher *PCNA* gene expression were observed compared with HFD WT (Fig. 4A, B). In HFD KO, the number of apoptotic cells demonstrated by TUNEL assay was reduced compared to HFD WT pregnant mice (Fig. 4C).

Next, we investigated autophagy in placenta tissues by electron microscopy. Most of autophagy activities were found in junctional zone, where increased autophagosomes as well as lysosomes were observed in HFD KO compared to HFD WT mice. However, the number of autophagolysosome was not increased in HFD KO mice, suggesting the impairment of autophagolysosome formation in HFD KO mice (Fig. 5A, B). Autophagosome formation and impaired clearance in HFD KO pregnant mice was reflected by accumulation of p62, microtubule-associated protein1 light chain 3 (LC3)-II, and lysosome-associated membrane protein 2 (LAMP2). Elevated insulin and glucose levels of HFD KO pregnant mice significantly activated phosphorated mTOR signalling, which is central regulator of autophagy and thereby induced autophagy dysfunction (Fig. 5C, Supplementary Figs. S4 and S5).

Increased tissue-resident decidual natural killer (trNK) cells in HFD KO placenta

The trophoblast cells interact with trNK cells via secreting Gal-9, its binding to CD366 (T-cell immunoglobulin domain and mucin domain-containing molecule-3; Tim-3) expressed on trNK cell, and suppressing cytotoxic immune responses of trNK cells at the maternal-fetal interface[10]. Although percentage of $CD45^+$ $CD3^-$ $CD49b^+$ conventional NK (cNK) cells was not altered, $CD45^+$ $CD3^-$ $CD49b^-$ $CD49a^+$ trNK cells was significantly increased in HFD KO compared with HFD WT placenta at GD19 (Fig. 6A, B and Supplementary Fig. S6A). In addition, the percentage of $CD45^+$ $CD3^-$ $CD49b^-$ $CD49a^+$ $C366^+$ (Tim-3^+) trNK cells significantly increased (Fig. 6C) and $CD45^+$ $CD3^-$ $CD49b^-$ CD49a + $C366^+$ $Zombie^-$ $Annexin^+$ early apoptotic trNK cells significantly decreased in HFD KO compared with HFD WT placenta (Fig. 6D and Supplementary Fig. S6B). The reduced expression of Gal-9 in HFD KO placenta may induce cytotoxic immune responses of trNK cells and it was demonstrated by upregulated expression of *Il10*, *Tnfa*, and *Eomes*, transcription factor that is known to be important in maturation and cytotoxic function of NK cells, while the expression of *Havcr2* and *Cd244* was unaltered (Fig. 6E). Since Gal-9 from trophoblasts activates the $CD11c^{high}$ decidual macrophages[8], we further investigated the M1/M2 macrophages in placenta. The percentage of $F4/80^+$ $CD11b^+$ macrophages and M1/M2 ratio ($F4/80^+$ $CD11b^+$ $CD86^+$ $CD163^-$ / $F4/80^+$ $CD11b^+$ $CD163^+$ $CD86^-$) were not altered between HFD KO and HFD WT placenta (Supplementary Fig. 6C–E).

Discussion

In our clinical observation study, plasma Gal-9 levels at 3rd trimester demonstrated positive correlation with HbA1c, placental weight and neonatal BW, although mRNA expressions of *LGALS9* were not altered in decidua and chorion of placenta from the pregnant women with GDM. The obtained placenta tissues are 5 in NGT and 5 in GDM groups and it is one of the limitations of the current investigation. Circulating Gal-9 levels were lower in non-pregnant women compared to the pregnant women with NGT and GDM. We also observed marked elevation of plasma Gal-9 levels during the 3rd trimester in GDM. This temporal elevation of Gal-9 may serve as a potential biomarker for fetal macrosomia. In the previous study, serum Gal-9 levels were not changed by comparing just before and after delivery in both the healthy and GDM groups[16]. It suggested circulating Gal-9 levels are temporally elevated during the 3rd trimester and go down to the lower levels before the delivery.

In general, Gal-9 is abundantly expressed and remained in cytoplasm in various tissues and cells; however, it is secreted out by non-classical pathway as damage-associated molecular patterns (DAMPs) or pathogen-associated molecular patterns (PAMPs), interacts as a ligand with Tim-3, and induces apoptosis of activated Th1 and Th17 cells[17]. The abundant mRNA expression in placenta and the elevated plasma concentrations of Gal-9 in GDM suggested its importance in the development of maternal and fetal complications. However, it was unexplored whether the elevated Gal-9 is hazardous or protective in the maintenance of pregnancy in GDM. Thus, we further proceeded to the experiments using B6-$Lgals9^{tm1glp}$ (KO) pregnant mice fed with HFD. In HFD

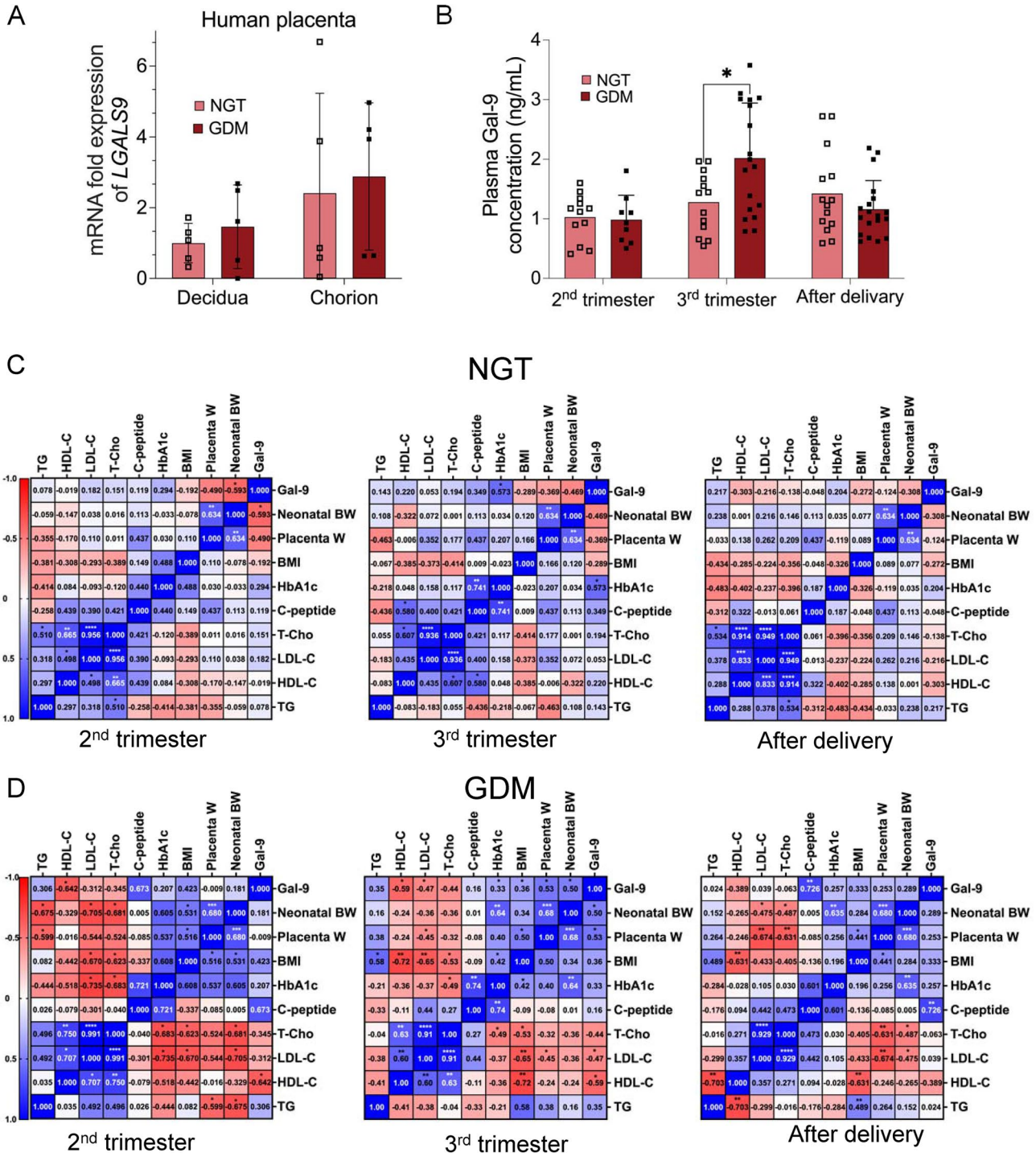

Fig. 1. Galectin-9 in pregnant women with normal glucose tolerance (NGT) and gestational diabetes mellitus (GDM). (**A**) *LGALS9* mRNA expression in decidua and chorion tissues of human placenta in NGT ($n = 5$) and GDM ($n = 5$). (**B**) Plasma Gal-9 concentrations in NGT ($n = 14$) and GDM ($n = 19$) at 2nd trimester, 3rd trimester, and after delivery. Data are shown as mean ± SD and analyzed by unpaired *t*-tests. **C**. Pearson correlation coefficient of plasma Gal-9 with various clinical parameters in NGT ($n = 14$) and GDM ($n = 19$) at 2nd trimester, 3rd trimester, and after delivery. ($^{*}p < 0.05$, $^{**}p < 0.01$, $^{***}p < 0.001$)

KO, the maternal impaired glucose tolerance and increased fetus weight were observed. Western blot analyses showed protein expression of Gal-9 increased in placenta, and it suggested that the compensatory elevation of Gal-9 in the placenta tissues of GDM. We failed to measure circulating Gal-9 levels by ELISA assay because of the limitation of blood samples. In previous study, the increased plasma Gal-9 levels at 1st trimester predicted the onset of subsequent preeclampsia and placenta and plasma Gal-9 levels were elevated in 3 independent

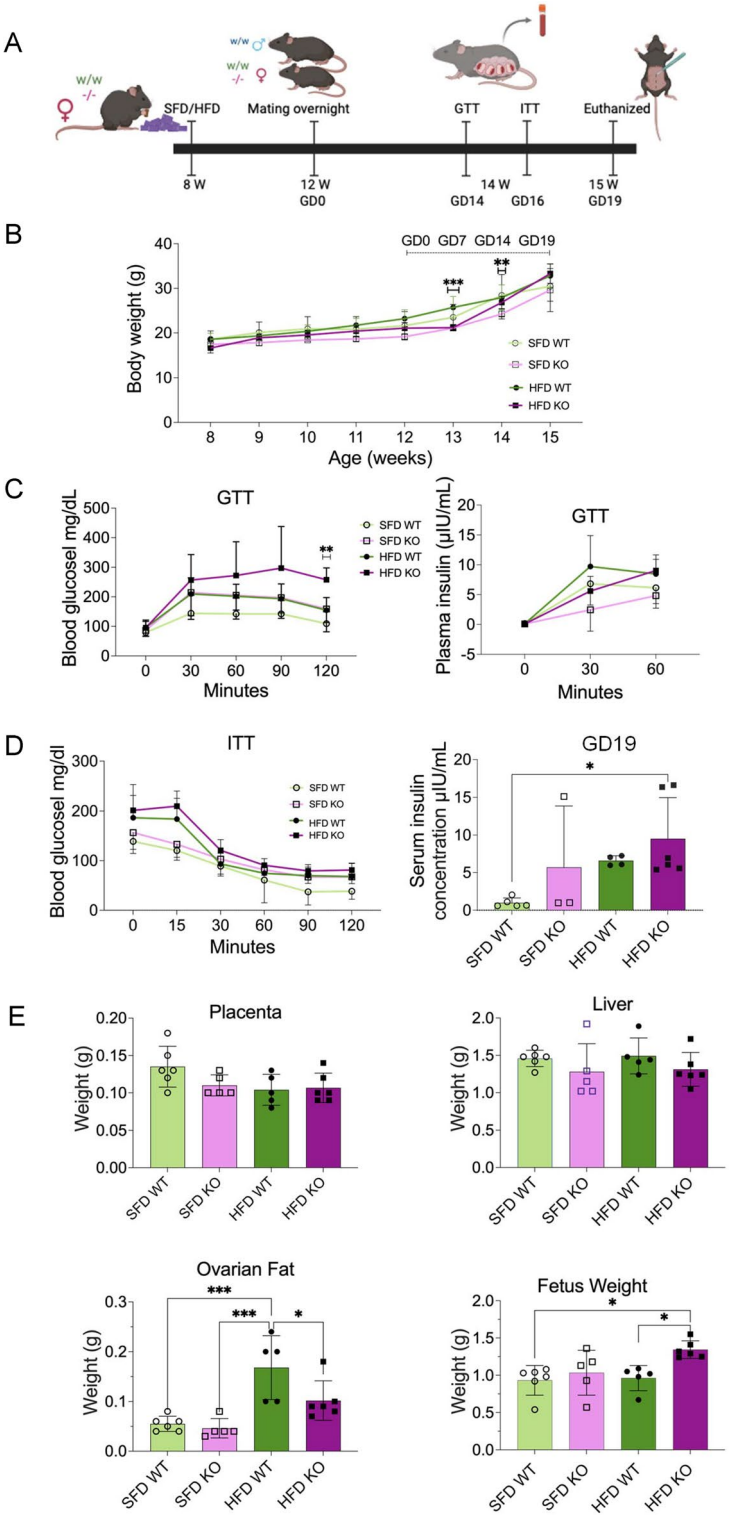

preeclampsia mouse models[8]. In contrast to our knockout mice experiments, the administration of Gal-9 induced the preeclampsia phenotype and Gal-9 blockade prevented the phenotype. Although the authors demonstrated the Gal-9 derived from trophoblast cells activated CD11c^{high} decidual macrophages and impaired spiral artery remodeling[8], there must be a distinct role and mechanism of Gal-9 in GDM. Human placenta lactogen (hPL), estrogen, progesterone and cortisol are known placenta-derived hormones which induce insulin resistance in pregnancy. Since progesterone favors NK cell activity that is necessary for the successful remodeling and angiogenesis and limits the migration and functions of conventional T cells, neutrophils and macrophages in the decidua[18], we preferentially measured progesterone levels and observed a non-significant increase in HFD KO. By the limitation of blood samples, we could not measure hPL, estrogen, and cortisol but future investigation is required.

◀**Fig. 2**. Glucose metabolism in B6-Lgals9^{tm1glp} (KO) and wild type (WT) pregnant mice. (**A**) Experimental design. WT (w/w) and KO (-/-) female mice were fed with standard fat diet (SFD, 10% fat) or high fat diet (HFD, 60% fat) and mated with WT male mice. GD, gestational day; W, weeks of age; GTT, glucose tolerance test; ITT, insulin tolerance test. Created in BioRender. H, H. (2025) (**B**) Body weight of SDF WT ($n=14$), SDF KO ($n=10$), HFD WT ($n=15$), and HFD KO ($n=9$) pregnant mice. Body weight in HFD KO mice at GD7 (21.18 ± 0.69 g) was significantly lower than HFD WT mice (25.71 ± 2.43) ($P=0.0005$). The body weight in SFD KO mice at GD14 (24.23 ± 1.09) was lower than SFD WT (28.41 ± 4.68) ($P=0.0025$). (**C**) Glucose levels [SFD WT ($n=7$), SFD KO ($n=5$), HFD WT ($n=8$), and HFD KO ($n=6$)] and plasma insulin levels [SFD WT ($n=6$), SFD KO ($n=5$), HFD WT ($n=5$), and HFD KO ($n=6$)] in GTT at GD14. (**D**) Glucose levels [SFD WT ($n=7$), SFD HFD ($n=8$), SFD KO ($n=5$), and HFD KO ($n=7$)] in ITT at GD16 and serum fasting insulin levels [SFD WT ($n=6$), SFD KO ($n=4$), HFD WT ($n=4$), and HFD KO ($n=6$)] at GD19. (**E**) Placenta, liver, ovarian fat and fetus weight of WT and KO pregnant mice fed with SFD or HFD at GD19. Data are shown as mean ± SD and analyzed by one-way ANOVA with Tukey test (*$p<0.05$, **$p<0.01$, ***$p<0.001$).

In HFD WT, Western blot analyses showed protein expression of Gal-9 increased in placenta, and immunohistochemistry demonstrated that the trophoblast giant cells (TGC) and spongiotrophoblasts (SP) in decidua and junctional zone expressed Gal-9. In HFD KO, trophoblast cell proliferation activity increased shown by PCNA stain and PCNA mRNA quantification, while the apoptotic activity decreased. Gal-9 was reported to maintain the autophagic function via co-operation with lysosomes by binding to N-glycosylated Asn^{175} of lysosome-associated membrane protein 2 (LAMP2)[15]. In placenta of HFD KO, p-mTOR, the number of autophagosome, and the number of lysosomes increased, while the number of autophagolysosome was reduced compared to HFD WT. It suggested that the regulation of cell cycle and autophagy function was impaired by the reduction of Gal-9 in placenta.

In human normal pregnancy, dNK cells are known to interact with the fetus by human leukocyte antigen (HLA) ligands on extravillous trophoblast cells to mediate the immune tolerance in the interphase of mothers and fetuses, and secrete various growth factors and cytokines, such as interferon (IFN)-γ, vascular endothelial growth factor (VEGF) and interleukin (IL)-8, to promote vascular remodeling, trophoblast invasion and fetal development[19]. In the patients with GDM, scRNA-seq demonstrated that the number of NK cells and cytotoxic T cells increased associated with an enhancement of CD206 + M2 macrophages[20]. Although the number of cNK cells in HFD KO were not altered, the number of trNK cells significantly increased in placenta compared with HFD WT. In the previous study in the patients with type 2 diabetes (T2D), the number of circulating NK cells and their expression of Tim-3 increased, and the expression of Tim-3 on NK cells correlated positively with HbA1c and negatively with total NK cell numbers[21]. In HFD KO, Tim-3 + trNK cells increased and early apoptotic trNK cells were significantly reduced. It suggests that reduction of Gal-9 from trophoblast cells failed to induce apoptosis of GDM-induced Tim-3 + trNK cells and it was associated with increased expression of inflammatory cytokines such as tumor necrosis factor (TNF)-α. We clearly demonstrated the deleterious effects of Gal-9 deficiency in maternal glucose intolerance and macrosomia during the later stage of pregnancy in mice at GD19 and suggested the compensation elevation of plasma Gal-9 levels at 3rd trimester of the pregnancy with GDM. The roles of Gal-9 expressed in trophoblasts are different in early vs. later phases of pregnancy and preeclampsia vs. GDM. In the early phase of normal pregnancy, Tim-3 is expressed on over 60% of dNK cells and Gal-9 produced by trophoblasts induces transformation of peripheral NK cells into dNK cells, increases IL-4, reduced TNF-α by the interaction with Tim-3[10]. In addition, Tim-3 + dNK cells demonstrated less cytotoxicity against Gal-9 expressing trophoblast cells in pregnant women[22]. The excess of Gal-9 positive cells and reduced Tim-3 positive cells in dNK cell population was observed in early-onset preeclampsia[11], and Gal-9 administration in 3 independent preeclampsia mouse models induced preeclampsia-like phenotypes[8].

In conclusion, plasma Gal-9 levels at 3rd trimester may be a biomarker for the prediction of maternal glucose intolerance and fetal macrosomia in pregnant women with GDM. In HFD KO, maternal impaired glucose tolerance and increased fetus weight, macrosomia, were observed. In the placenta derived from HFD KO, increased proliferation, reduced apoptosis, and impaired autophagy function of trophoblast cells were observed. In addition, Tim-3 + trNK cells increased and early apoptotic trNK cells were significantly reduced and inflammatory responses with increased expression of *Tnfa* and *Eomes* were observed. It suggested the reduction of Gal-9 from trophoblast cells failed to provoke apoptosis of GDM-induced Tim-3 + trNK cells (Supplementary Fig. S7).

Materials and methods

Observational clinical study

Plasma samples were collected at 2nd trimester (24–26 gestational weeks) 3rd trimester (34–38 gestational weeks) and 3–5 days after delivery from pregnant women; 14 women with normal glucose tolerance (NGT) and 19 women with gestational diabetes mellitus (GDM). Plasma was also collected from 10 non-pregnant women. Placenta tissues ($n=5$ in NGT and $n=5$ in GDM groups) were obtained at Okayama University Hospital. The clinical study was approved by Ethics Committee, Okayama University Hospital (#1910-015). The informed consent was obtained from all subjects, and clinical study was performed in accordance with the Declaration of Helsinki.

Animal experiments

We obtained B6-Lgals9^{tm1glp} (KO) from Dr. Mitsuomi Hirashima at Kagawa University and C57BL/6J mice from Japan Charles River. Eight-week-old female mice were randomly assigned to standard fat diet group (SFD)

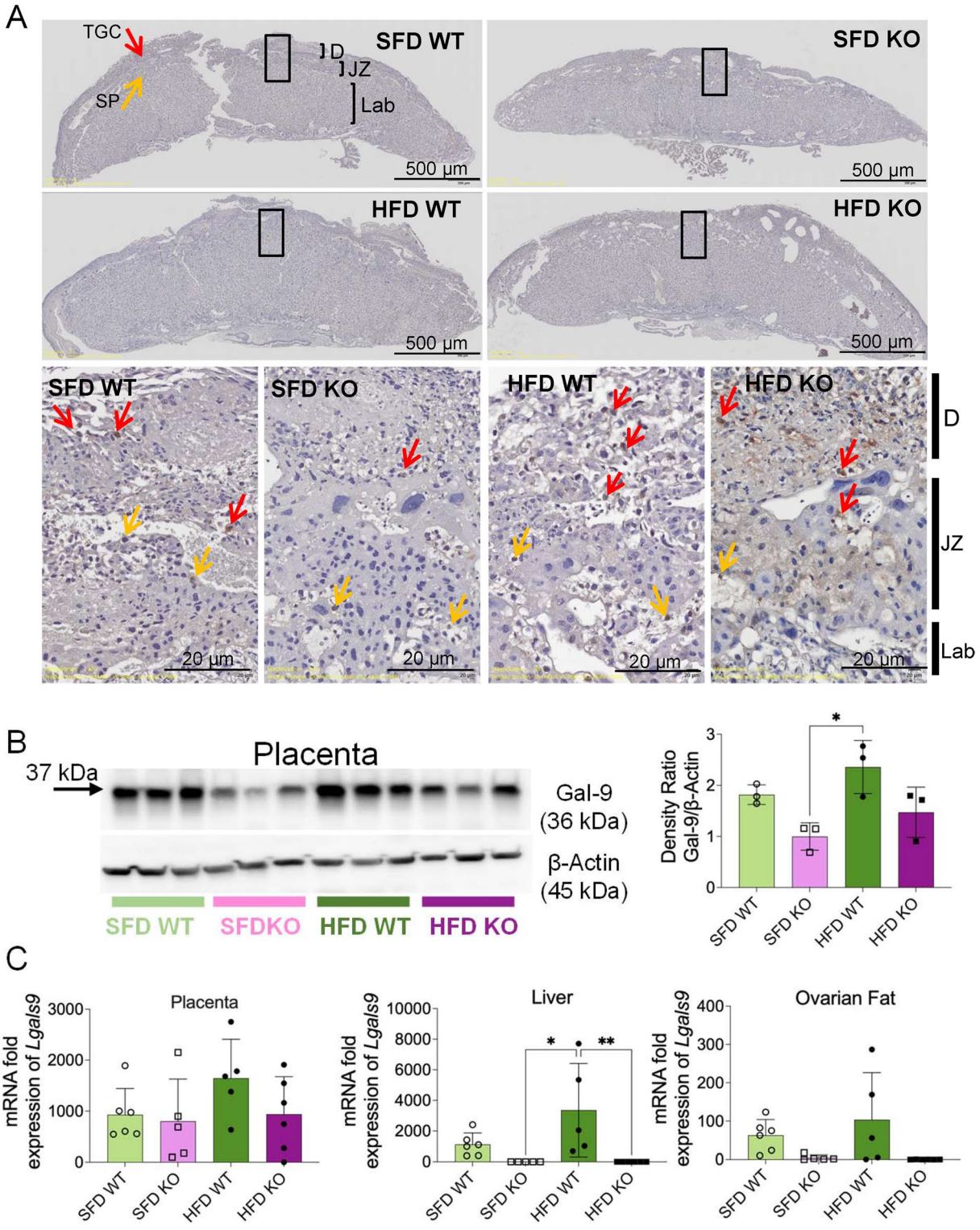

Fig. 3. Expression of Gal-9 in placenta derived from B6-Lgals9^{tm1glp} (KO) and wild type (WT) pregnant mice. (**A**) Immunohistochemical staining of Gal-9 in placenta at gestational day (GD19). Gal-9 is observed in the cytoplasm and cell surface of trophoblast giant cells (TGC, red arrows) and spongiotrophoblast cells (SP, yellow arrows) in SFD WT, SFD KO, HFD WT, and HFD KO mice. D, decidua; JZ, junctional zone; Lab, labyrinth. **B**. Western blot analysis of Gal-9 in placenta at GD19 and densitometric analyses ($n = 3$ in each group). **C**. mRNA expression of *Lgals9* normalized by *Rplp0* and *Gapdh* in placenta, liver, and ovarian fat derived from SFD WT ($n = 6$), SFD KO ($n = 5$), HFD WT ($n = 5$), and HFD KO ($n = 6$). Data are shown as mean ± SD and analyzed by one-way ANOVA with Tukey test (*$p < 0.05$; **$p < 0.01$). SFD, standard fat diet, 10% fat; HFD, high fat diet, 60% fat.

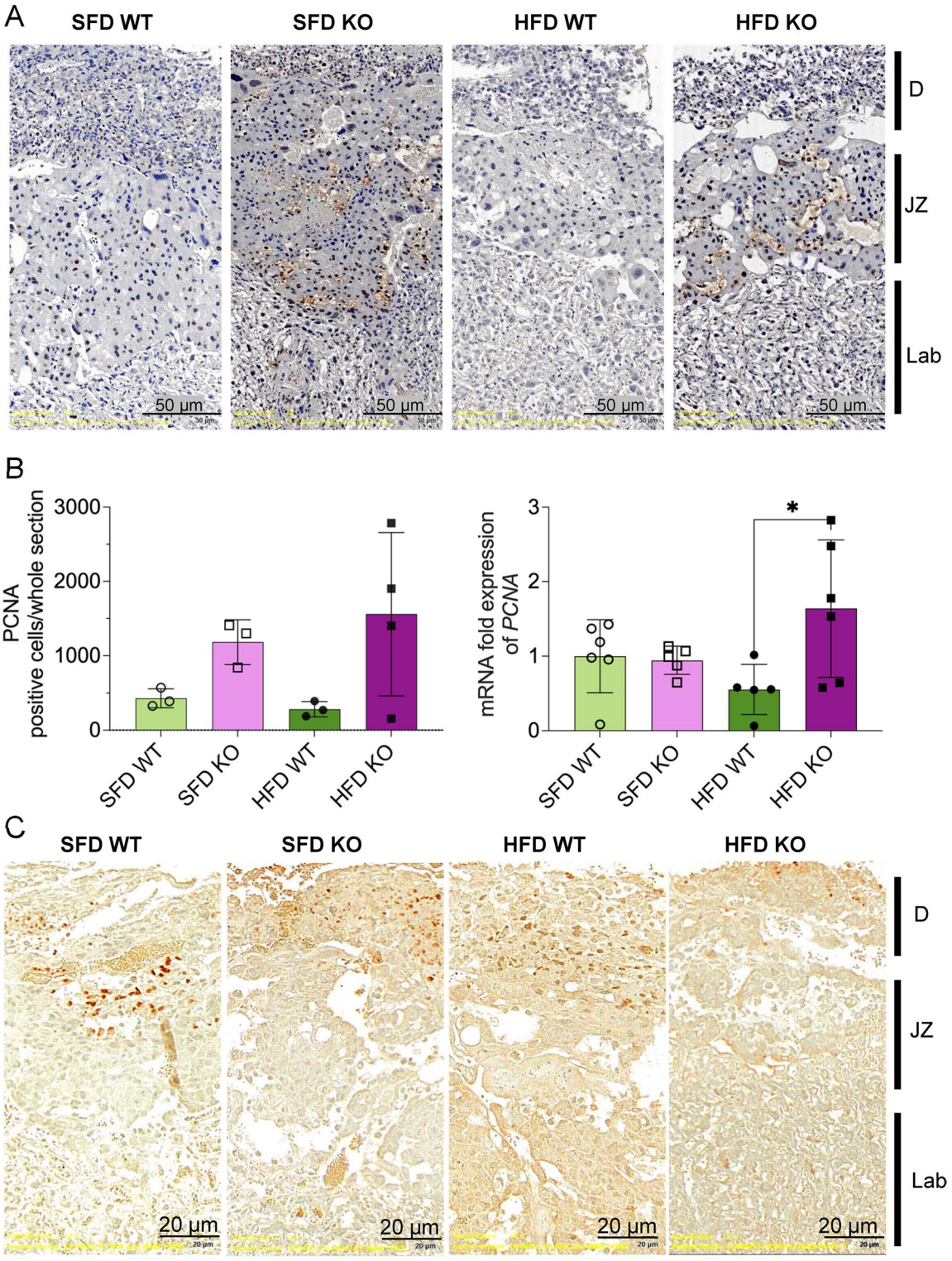

Fig. 4. Proliferating cell nuclear antigen (PCNA) and apoptosis assay in placenta derived from B6-Lgals9^{tm1glp} (KO) and wild type (WT) pregnant mice. (**A**) Immunohistochemical staining of PCNA in placenta at gestational day 19 (GD19). (**B**) The counts of PCNA positive cells in whole placenta sections in SFD WT ($n=3$), SFD KO ($n=3$), HFD WT ($n=3$), and HFD KO ($n=4$), and mRNA expression of *Pcna* normalized by *Rplp0* in SFD WT ($n=5$), SFD KO ($n=5$), HFD WT ($n=5$), and HFD KO ($n=6$). (**C**) Terminal deoxynucleotidyl transferase dUTP nick-end labeling (TUNEL assay) of placenta at GD19. The apoptotic cells are labeled by 3,3′-Diaminobenzidine (DAB). SFD, standard fat diet, 10% fat; HFD, high fat diet, 60% fat.

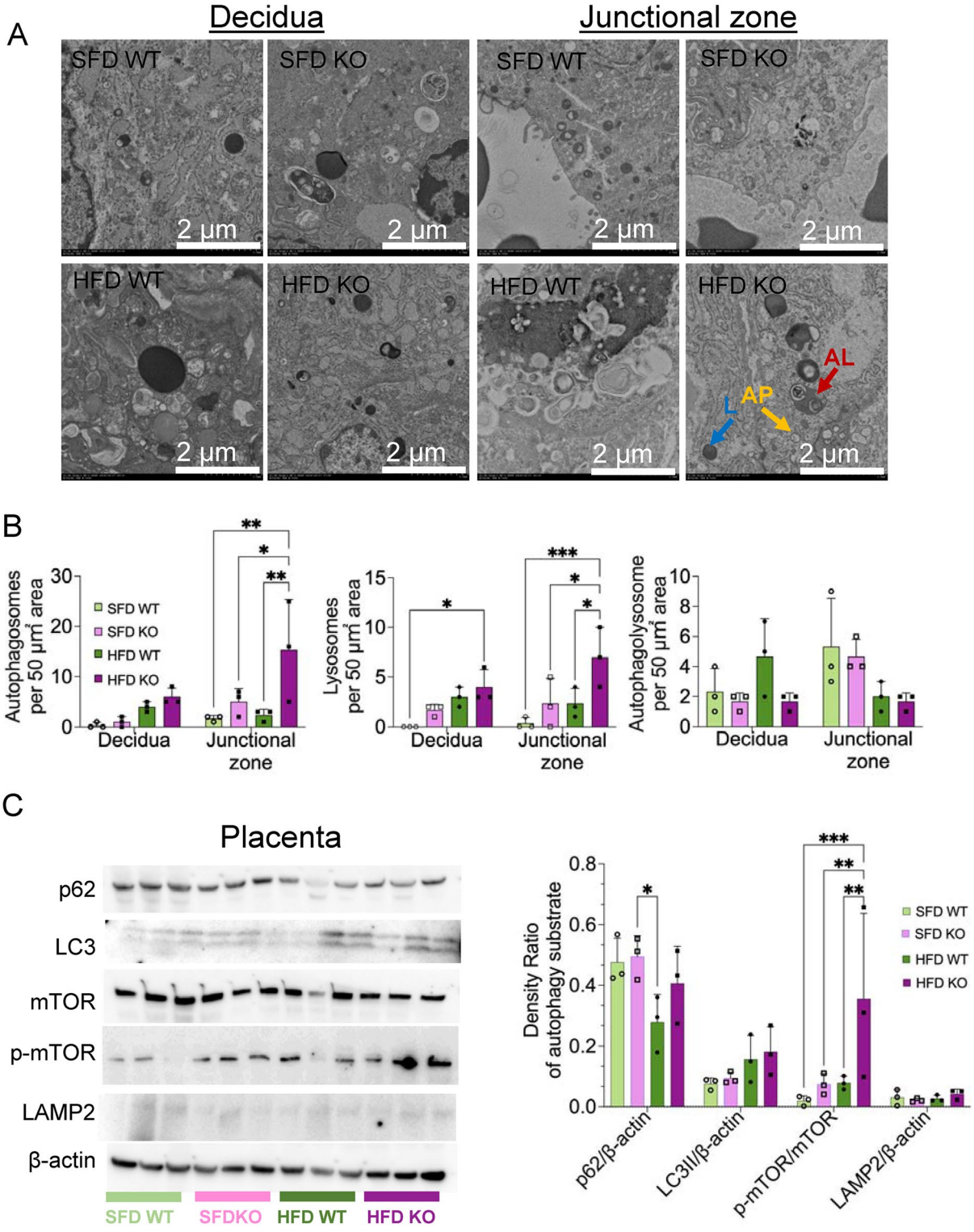

Fig. 5. Autophagy in placenta derived from B6-Lgals9^{tm1glp} (KO) and wild type (WT) pregnant mice. (**A**) Electron micrographs of placenta at gestational day 19 (GD19) showing decidua and junctional zone. AP, autophagosome (yellow arrow); L, lysosomes (blue arrow); AL, autophagolysosomes (red arrow). (**B**) The number of autophagosome, lysosomes and autolysosomes per 50 µm2 area of decidua and junctional zone. (**C**) Western blots and densitometric analyses of p62, microtubule-associated protein 1 A/1B-light chain 3 (LC3), mammalian target of rapamycin (mTOR), phosphorylated mTOR (p-mTOR) and β-actin. Data shown as mean ± SD and analyzed by one-way ANOVA with Tukey test (*$p < 0.05$, **$p < 0.01$ and ***$p < 0.001$). SFD, standard fat diet, 10% fat; HFD, high fat diet, 60% fat.

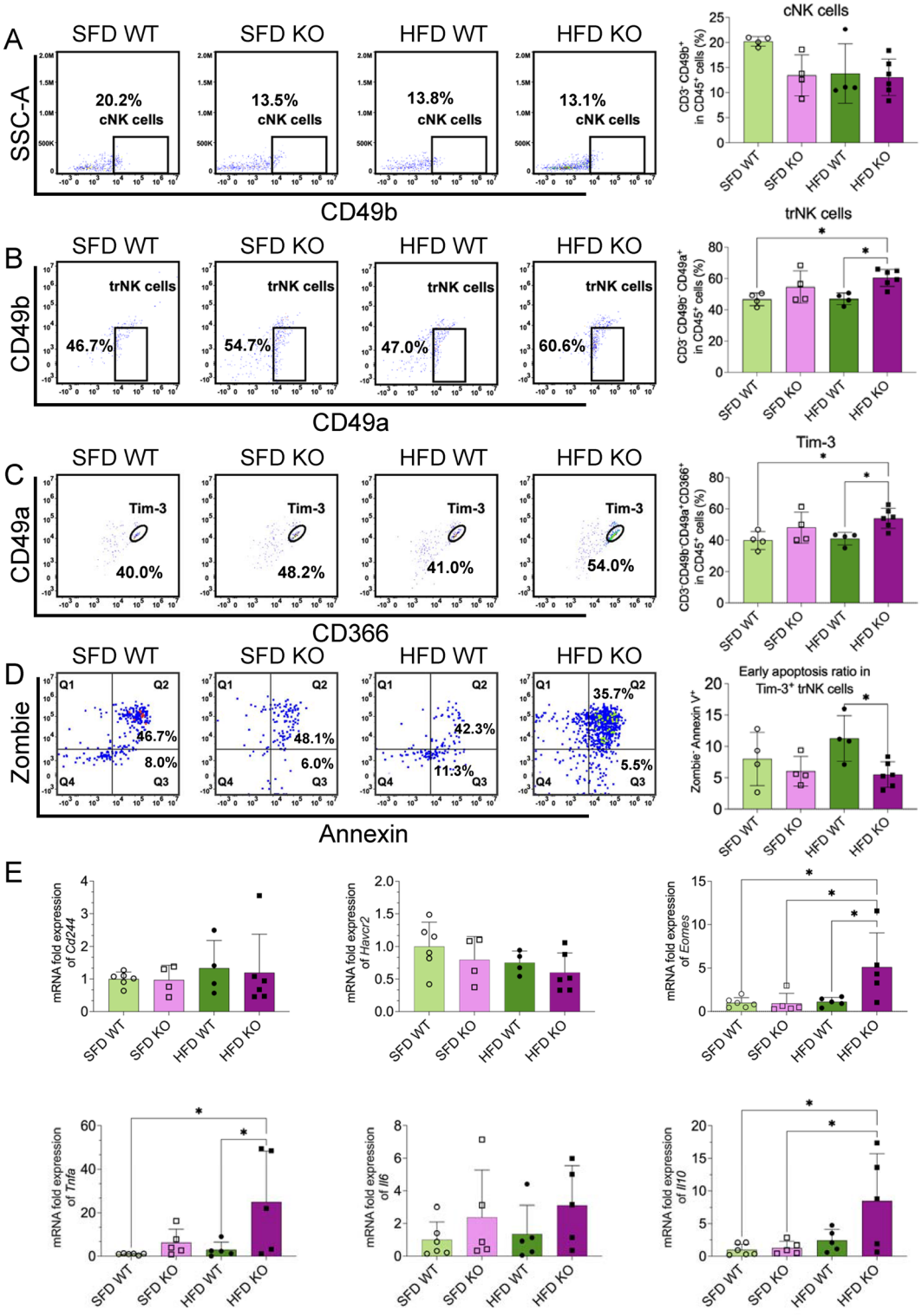

Fig. 6. Flow cytometry analysis in placenta derived from B6-Lgals9^{tm1glp} (KO) and wild type (WT) pregnant mice. (**A**) Percentage of CD45$^+$ CD3$^-$ CD49b$^+$ conventional NK (cNK) cells in total leukocytes. (**B**) Percentage of CD45$^+$ CD3$^-$ CD49b$^-$ CD49a$^+$ trNK (tissue-resident NK) cells in total leukocytes. (**C**) Percentage of CD45$^+$ CD3$^-$ CD49b$^-$ CD49a$^+$ C366$^+$ (Tim-3$^+$) trNK cells. Tim-3, T-cell immunoglobulin domain and mucin domain-containing molecule-3. (**D**) Percentage of Zombie$^-$ Annexin$^+$ early apoptotic trNK cells in Tim-3 + trNK cells. (**E**) mRNA expression of *Cd244*, *Havcr2* (Tim-3), *Eomes*, *Tnfa*, *Il6*, and *Il10*. Data shown as mean ± SD and analyzed by one-way ANOVA with Tukey test (*$p < 0.05$). $N = 4–6$ in each group. SFD, standard fat diet, 10% fat; HFD, high fat diet, 60% fat.

fed with 10 kcal% fat (Cat# D12450J, Research Diets, New Brunswick, NJ) or high fat diet group (HFD) fed with 60 kcal% (Cat# D12492, Research Diets). At 12 weeks of age, male C57BL/6J mouse ($n=1$) and female mice ($n=2$) were mated overnight. The vaginal mucous plugs were confirmed, female mice housed in separated cages and designated as gestation day 0 (GD0). We performed glucose tolerance test (GTT) at GD14 and insulin tolerance test (ITT) at GD16. At GD19, fetus and various organs from pregnant mice were obtained and subjected to following experiments (Fig. 1C). All animal experiments were approved by the Animal Care and Use Committee of the Department of Animal Resources, Advanced Science Research Center, Okayama University (OKU-2023016). All animal experiments were carried out in accordance with relevant guidelines and regulations. The study is reported in accordance with ARRIVE guidelines.

Glucose tolerance test and insulin tolerance test (GTT and ITT)

At GD14 (5–8 individual mice from each experimental group) were fasted for 16 h in GTT and for 4 h in ITT in GD16 from 5 to 6 individual mice from each experimental group. They were then intraperitoneally injected with glucose solution (2 mg/g body weight) and human insulin (1 unit/kg in HFD groups and 0.75 unit/kg in SFD groups) for GTT and ITT, respectively.

Plasma levels of galectin-9, insulin and progesterone

Human Galectin-9 ELISA Kit - Quantiline (R&D systems, Minneapolis, MN), LBIS Mouse Insulin ELISA Kit (High Sensitivity) (Fuji Film, Osaka, Japan) and Elecsys Progesterone III (Roche diagnostics, Rotkreuz, Switzerland) were used plasma levels of galectin-9 (Gal-9) in human, insulin and progesterone in mice, respectively. We calculated insulin resistance index by HOMA-β, HOMA-IR, and insulinogenic index as follows.

Insulinogenic index = ΔIRI (30 min–0 min)(μU/mL)/Δblood glucose (30 min–0 min)(mg/dL).

HOMA-β = fasting IRI (μU/mL)×360/[fasting glucose (mg/dL)-63]

HOMA-IR=[fasting IRI (μU/mL)×fasting glucose (mg/dL)/405.

Immunohistochemistry and TdT-mediated dUTP Nick end-labeling (TUNEL) assay

Mouse placenta tissues ($n=4$) were taken from each experimental group, fixed in 10% formaldehyde, then embedded in paraffin, and sectioned at thickness of 5 μm. They were deparaffinized, rehydrated and pretreated by microwave for 10 min in citrate buffer, pH 6.0. Endogenous peroxidase activity was blocked by 3% hydrogen peroxide. Nonspecific binding was blocked by incubation in 10% goat serum for 30 min. The tissue sections were incubated with purified anti-mouse galectin-9 (Biolegend Cat# 137901, RRID: AB_10568691, 1:100) and anti-PCNA (D3H8P) XP Rabbit mAb (Cell Signaling Technology Cat# 13110, RRID: AB_2636979, 1:8000) at 4 °C overnight. After being washed in PBS, they were incubated with Goat anti-Rat IgG H&L (HEP) (Abcam Cat# ab97057, RRID: AB_10680316) and SingalStain Boost IHC Detection Reagent (HRP, Rabbit) (Cell Signaling Technology Cat# 8114, RRID: AB_10544930) as secondary antibodies, respectively. The immunoreactivities were visualized by ImmPACT DAB Substrate Kit, Peroxidase (HRP) (Vector Laboratories Cat# SK-4105, RRID: AB_2336520). In situ Apoptosis Detection kit (Takara Bio Cat# MK500, RRID: AB_2800362), was used for TUNEL assay in mouse placenta tissues. All images were captured using Olympus BX61VS Virtual Slide Microscope (Olympus, Tokyo, Japan) and analyzed by Image J.

Reverse transcription-quantitative polymerase chain reaction (RT-qPCR)

RNAs were extracted from decidua and chorion of human placenta, and mouse frozen tissues with RNeasy Mini kit (Qiagen). For gene expression analyses, cDNAs were prepared with High-Capacity RNA-to-cDNA Kit (Applied Biosystems). TaqMan gene expression primers, human *LGALS9* (Hs04190742_mH), human *GAPDH* (Hs02786624_g1), mouse *Lgals9* (Mm00495295_m1), mouse *Gapdh* (Mm99999915_g1), *Rplp0* (Mm00725448_s1), mouse *Pcna* (Mm05873628_g1), mouse *Lamp1* (Mm01217070_m1), mouse *Eomes* (Mm01351986_m1), mouse *Tnf* (Mm00443258_m1), mouse *Il6* (Mm00446190_m1), mouse *Il10* (Mm00439614_m1), mouse *Havcr2* (Mm01294183_m1), and mouse *Cd244* (Mm00479575_m1) were used (Thermo Fisher Scientific). *Rplp0* and *Gapdh* were served as invariant controls. The RT-qPCR was performed using TaqMan Universal PCR Master mix II (with UNG) by using a StepOne Plus Real-Time PCR system. The quantification was performed by the $2^{-\Delta\Delta CT}$ analysis methods.

Transmission electron microscope (TEM)

Mouse placentae were dissected, and specific layers of decidua and junctional zone were isolated. They were immersed in 2.5% glutaraldehyde for 2 h at 4 °C and subsequently fixed with 1% osmium tetroxide. The samples were then subjected to dehydration, EPON embedding, and ultrathin sectioning. The four serial ultrathin sections were set on a grid and observed under an electron microscope (H7650, Hitachi, Tokyo, Japan).

Western blot analysis

Protein extracted from mouse placenta by Minute Total Protein Extraction Kit for Animal Cultured Cells and Tissues (Invent Biotechnologies). The samples were boiled in SDS-PAGE loading buffer, separated on 12% and 4–20% Mini-PROTEAN TGX Precast Protein Gels (Bio-Rad), and transferred to a PVDF Blotting Membrane (Cytiva). After blocking with 5% nonfat milk for 1 h at room temperature, the blots were incubated with Purified anti-mouse Galectin-9 (BioLegend Cat# 137901, RRID: AB_10568691) and subsequently with Goat Anti-Rat IgG H&L (HRP) (Abcam Cat# ab97057, RRID: AB_10680316) as a secondary antibody. Anti-p62 (SQSTM1) (Human) pAb (Polyclonal Antibody) (MBL International Cat# PM045, RRID: AB_1279301), Anti-Human LC3 Polyclonal Antibody (MBL International Cat# PM036, RRID: AB_2274121), mTOR (7C10) Rabbit mAb (Cell Signaling Technology Cat# 2983, RRID: AB_2105622), Phospho-mTOR (Ser2448) Antibody (Cell Signaling Technology Cat# 2971, RRID: AB_330970), LAMP2b antibody [EPR4207(2)] (Abcam Cat# ab125068, RRID:

AB_10971511), and β-Actin (13E5) Rabbit mAb (Cell Signaling Technology Cat# 4970, RRID: AB_2223172) as an internal loading control were also incubated with the blots overnight at 4 °C. After washing three times with Tris-buffered saline (TBS), the blots were incubated with Donkey Anti-Rabbit IgG, Whole An ECL Antibody, HRP-Conjugated (Cytiva Cat# NA934, RRID: AB_772206, 1:100000) at RT for 1 h. The blots were developed with Pierce ECL Western Blotting Substrate (Thermo Fisher Scientific). The chemiluminescence was analyzed using ImageQuant LAS-4000 mini (FUJIFILM).

Flow cytometer analysis of tissue-resident decidual natural killer cells (trNK)

Tissue collection and leukocyte isolation were performed as described[23]. In brief, we collected 2–3 placenta weighting 100–150 mg at gestational day 19 (GD19) and placenta tissues were subjected to mechanical dissociation and enzymatic digestion with StemPro Accutase Cell Dissociation Reagent (Life Technologies Cat# A1110501). The samples were then incubated horizontally in a 37 °C incubator for 30–35 min with gentle shaking (80 rpm). The cell suspension was poured through a 100 μm strainer into 50 mL tubes, washed by PBS, and centrifuged (1,300 *g* and 4 °C) for 10 min. After the removal of the supernatant, the cell pellet was resuspended in 1 mL RPMI without FBS (fetal bovine serum) and slowly overlaid on top of 500 μL of FBS, centrifuged (1,300 *g*, room temperature; RT) for 10 min. The cell pellet was again resuspended in 1 mL RPMI without FBS, layered on the 1 mL of Lympholyte Cell Separation Media (Cedarlane Cat# CL5031), and centrifuged (500 *g* and RT) for 30 min. The mononuclear cells were carefully removed from the interface, washed in PBS, and 1×10^6 cells were stained with 100 μL of 1:500 diluted Zombie Violet dye (BioLegend Cat# 423113) at RT in dark for 10–15 min. The cells were washed once by 500 μl of Cell Staining Buffer (BioLegend Cat# 420201), centrifuged at 1,300 *g* for 10 min. The cells were mixed gently with the following antibodies with 1:100 dilution in Cell Staining Buffer: PE anti-mouse CD45 (BioLegend Cat# 103105, RRID: AB_312970), FITC anti-mouse CD3 (BioLegend Cat# 100203, RRID: AB_312660), APC/Cyanine7 anti-mouse CD49b (pan-NK cells) (BioLegend Cat# 108919, RRID: AB_2561457), PE/ Cyanine7 anti-mouse CD49a (BioLegend Cat# 142607, RRID: AB_2749930), PerCP/Cyanine5.5 anti-mouse CD366 (Tim-3) (BioLegend Cat# 134011, RRID: AB_2632735), and incubated at RT in dark for 15–20 min. The cells were washed by adding 500 μL of Cell Staining Buffer, centrifuged at 1300 *g* for 10 min and resuspended in Annexin V Binding Buffer (BioLegend Cat# 422201). After the addition of 5 μL of APC-conjugated Annexin V (BioLegend Cat# 640919), they were incubated at RT in dark for 10–15 min. Following the addition of 400 μL of Annexin V Binding Buffer they were analyzed by CytoFLEX Flow Cytometer (Beckman Coulter, Brea, CA) and FlowJo (Tree Star, Ashland, OR).

Flow cytometer analysis of mouse placenta macrophages

The 1×10^6 leukocytes isolated from placenta described above were stained with 100 μL of 1:500 diluted Zombie Aqua (BioLegend Cat# 423101) at RT in dark for 10–15 min. The cells were stained with PE anti-mouse CD45 (BioLegend Cat# 103105, RRID: AB_312970), FITC anti-mouse F4/80 (BioLegend Cat# 123107, RRID: AB_893500), APC anti-mouse/human CD11b (BioLegend Cat# 101211, RRID: AB_312794), PE/Cyanine7 anti-mouse CD163 (BioLegend Cat# 155319, RRID: AB_2890710), PerCP/Cyanine5.5 anti-mouse CD86 (BioLegend Cat# 159211, RRID: AB_3106039), incubated at RT in dark for 15–20, and analyzed by flow cytometry.

Statistical analysis

All values were represented as the mean ± standard deviation (SD). Statistical analyses were conducted using GraphPad Prism (version 10). Student t-test, one-way ANOVA with Tukey and Holm-Šídák corrections were used to determine the differences. $p < 0.05$ was considered statistically significant.

Data availability

The experimental data and the simulation results that support the findings of this study are available in Figshare with the identifier https://doi.org/10.6084/m9.figshare.28451660. The corresponding author should be contacte d if someone wants to request the data from this study.

Received: 17 February 2025; Accepted: 22 May 2025
Published online: 30 May 2025

References

1. McElwain, C. J., McCarthy, F. P. & McCarthy, C. M. Gestational diabetes mellitus and maternal immune dysregulation: what we know so Far. *Int. J. Mol. Sci.* **22** (2021).
2. Sweeting, A., Wong, J., Murphy, H. R. & Ross, G. P. A clinical update on gestational diabetes mellitus. *Endocr. Rev.* **43**, 763–793 (2022).
3. Chen, M. et al. Galectins: important regulators in normal and pathologic pregnancies. *Int. J. Mol. Sci* **23** (2022).
4. Wada, J., Ota, K., Kumar, A., Wallner, E. I. & Kanwar, Y. S. Developmental regulation, expression, and apoptotic potential of galectin-9, a beta-galactoside binding lectin. *J. Clin. Invest.* **99**, 2452–2461 (1997).
5. Menkhorst, E. et al. Medawar's postera: galectins emerged as key players during Fetal-Maternal glycoimmune adaptation. *Front. Immunol.* **12**, 784473 (2021).
6. Meggyes, M. et al. Feto-maternal immune regulation by TIM-3/galectin-9 pathway and PD-1 molecule in mice at day 14.5 of pregnancy. *Placenta* **36**, 1153–1160 (2015).
7. Heusschen, R. et al. Profiling Lgals9 splice variant expression at the fetal-maternal interface: implications in normal and pathological human pregnancy. *Biol. Reprod.* **88**, 22 (2013).
8. Li, Y. et al. A Galectin-9-Driven CD11c(high) decidual macrophage subset suppresses uterine vascular remodeling in preeclampsia. *Circulation* **149**, 1670–1688 (2024).
9. Li, Z. H. et al. Galectin-9 alleviates LPS-Induced Preeclampsia-Like impairment in rats via switching decidual macrophage polarization to M2 subtype. *Front. Immunol.* **9**, 3142 (2018).

10. Li, Y. H. et al. The Galectin-9/Tim-3 pathway is involved in the regulation of NK cell function at the maternal-fetal interface in early pregnancy. *Cell. Mol. Immunol.* **13**, 73–81 (2016).
11. Miko, E. et al. Involvement of Galectin-9/TIM-3 pathway in the systemic inflammatory response in early-onset preeclampsia. *PLoS One*. **8**, e71811 (2013).
12. Hao, H. et al. Upregulation of the Tim-3/Gal-9 pathway and correlation with the development of preeclampsia. *Eur. J. Obstet. Gynecol. Reprod. Biol.* **194**, 85–91 (2015).
13. Hashemi, E., Malarkannan, S. & Tissue-Resident, N. K. Cells: Development, maturation, and clinical relevance. *Cancers (Basel)* **12** (2020).
14. Wang, W. et al. Galectin-9 targets NLRP3 for autophagic degradation to limit inflammation. *J. Immunol.* **206**, 2692–2699 (2021).
15. Sudhakar, J. N. et al. Lumenal Galectin-9-Lamp2 interaction regulates lysosome and autophagy to prevent pathogenesis in the intestine and pancreas. *Nat. Commun.* **11**, 4286 (2020).
16. Pelech, A. et al. Do serum galectin-9 levels in women with gestational diabetes and healthy ones differ before or after delivery? A pilot study. *Biomolecules* **13** (2023).
17. Zhu, C. et al. The Tim-3 ligand galectin-9 negatively regulates T helper type 1 immunity. *Nat. Immunol.* **6**, 1245–1252 (2005).
18. Shah, N. M., Lai, P. F., Imami, N. & Johnson, M. R. Progesterone-Related immune modulation of pregnancy and labor. *Front. Endocrinol. (Lausanne)*. **10**, 198 (2019).
19. Zhang, X. & Wei, H. Role of decidual natural killer cells in human pregnancy and related pregnancy complications. *Front. Immunol.* **12**, 728291 (2021).
20. Yang, Y. et al. Transcriptomic profiling of human placenta in gestational diabetes mellitus at the Single-Cell level. *Front. Endocrinol. (Lausanne)*. **12**, 679582 (2021).
21. Wang, H., Cao, K., Liu, S., Xu, Y. & Tang, L. Tim-3 expression causes NK cell dysfunction in type 2 diabetes patients. *Front. Immunol.* **13**, 852436 (2022).
22. Sun, J. et al. Tim-3 is upregulated in NK cells during early pregnancy and inhibits NK cytotoxicity toward trophoblast in Galectin-9 dependent pathway. *PLoS One*. **11**, e0147186 (2016).
23. Arenas-Hernandez, M., Sanchez-Rodriguez, E. N., Mial, T. N., Robertson, S. A. & Gomez-Lopez, N. Isolation of leukocytes from the murine tissues at the Maternal-Fetal interface. *J. Vis. Exp.*, e52866 (2015).

Acknowledgements

We acknowledge the animal care from Department of Animal Resources, Advanced Science Research Center, Okayama university. We also acknowledge technical support from Central Research Laboratory, Okayama University Medical School for the usage of CytoFLEX Flow Cytometer and producing paraffin blocks and sections.

Author contributions

H.A., M.W., and J.W. designed the project and experiments and wrote the manuscript. H.A., R.S., E.K., K.M., Y.O., B.Y., A.K., B.Y., K.M., A.K., T.T., I.N., A.N., and J.E. performed animal experiments, analyzed and interpreted data. M.W., J.M., E.E., K.H., and H.M. designed the clinical observational study of pregnant women with gestational diabetes and obtained clinical data and samples.

Declarations

Competing interests

Jun Wada receives speaker honoraria from Astra Zeneca, Bayer, Boehringer Ingelheim, Daiichi Sankyo, Kyowa Kirin, Novo Nordisk, and Mitsubishi Tanabe, and receives grant support from Bayer, Chugai, Kyowa Kirin, Otsuka, Shionogi, Sumitomo, and Mitsubishi Tanabe. All other authors have nothing to disclose.

Additional information

Supplementary Information The online version contains supplementary material available at https://doi.org/10.1038/s41598-025-03879-8.

Correspondence and requests for materials should be addressed to J.W.